J Solid State Electrochem (2012) 16:3341–3348
DOI 10.1007/s10008-012-1777-5

ORIGINAL PAPER

Electrostatic spray deposition of graphene nanoplatelets for high-power thin-film supercapacitor electrodes

Majid Beidaghi · Zhifeng Wang · Lin Gu · Chunlei Wang

Received: 11 April 2012 / Revised: 11 May 2012 / Accepted: 14 May 2012 / Published online: 26 May 2012

Abstract Thin-film electrodes of graphene nanoplatelets (GNPs) were fabricated through the electrostatic spray deposition (ESD) technique. The combination of a binder-free deposition technique and an open pore structure of graphene films results in an excellent power handling ability of the electrodes. Cyclic voltammetry measurements of 1-μm-thick electrodes yield near rectangular curves even at a very high scan rate of 20 V s^{-1}. Thin-film electrodes (1 μm thickness) show specific power and energy of about 75.46 kW kg^{-1} and 2.93 W h kg^{-1}, respectively, at a 5 V s^{-1} scan rate. For the thin-film electrode, about 53 % of the initial specific capacitance of electrodes at low scan rates was retained at a high scan rate of 20 V s^{-1}. Although the thickness of the thin-film electrodes has influence on their rate capability, an electrode with an increased thickness of 6 μm retained about 30 % if its initial capacitance at a very high scan rate of 20 V s^{-1}. The results show that the ESD-fabricated GNP electrodes are promising candidates for thin-film energy storage for applications that require moderate energy density and very high power and rate handling ability.

Keywords Thin-film electrodes · Electrostatic spray deposition · Supercapacitor · Graphene · High power density

M. Beidaghi · C. Wang (✉)
Department of Mechanical and Materials Engineering,
Florida International University,
Miami, FL 33174, USA
e-mail: wangc@fiu.edu

Z. Wang · L. Gu
Beijing National Laboratory for Condensed Matter Physics,
Institute of Physics, Chinese Academy of Science,
Beijing 100190, People's Republic of China

Introduction

Electrochemical capacitors (ECs), also called supercapacitors or ultracapacitors, are energy storage devices with higher energy densities than electrostatic or electrolytic capacitors and higher power densities compared to batteries [1]. ECs offer a combination of characteristics such as high-power density, long life cycle, wide working temperature range, and safety. These unique properties have made ECs an excellent choice for energy storage in applications such as portable electronics, uninterruptable power supplies, and automotive applications [2]. Based on the charge storage mechanism, ECs are of two types: electric double layer capacitors (EDLCs) which store charge by adsorption of electrolyte ions on the surface of an electrode with a high specific surface area. Different types of high-surface area carbon materials are usually used as electrode materials for EDLCs. Pseudo-capacitors store charge by faradic reactions that takes place on the surface or subsurface of the electrodes. Transition metal oxides and conducting polymers are examples of pseudo-capacitive materials [3]. Among all the desired properties of ECs, high power density, high-frequency response, and rate capability are very important for their future applications. These properties are particularly significant if the supercapacitors are to be used to provide the peak power in systems with batteries, fuel cells, or energy harvesters as the primary energy source. High-frequency response is the most important property for supercapacitors if they were to replace electrolytic capacitors in applications such as filtering voltage ripples in line-powered electronics (ac line filtering) [4]. Achieving a high-frequency response and rate capability is dependent on the various constituents of a supercapacitor including the electrode materials, electrolyte, and the method of assembly of materials on the current collectors.

Although pseudo-capacitive materials show promising energy density, the slow charge storage mechanism immensely impacts their power density and rate handling capabilities. On the other hand, EDLCs based on carbon materials show high-power density and can be charged and discharged in very short times [3, 5, 6]. Recently, single-layer and multilayer graphene nanosheets have attracted much research interest as electrode materials for supercapacitors. The specific capacitance of graphene nanosheets in the range of 38–264 F g^{-1} [7–10] depends on various factors including: preparation method, specific surface area, number of layers in the multilayer graphene, and the electrolyte, among others [7].

In the processes of fabricating supercapacitor electrodes, the method of depositing active materials on current collectors is one of the vital factors that affect the performance of the supercapacitor. Currently two kinds of electrode fabrication methods have been reported to prepare graphene supercapacitor electrodes based on the presence or absence of a polymeric binder to attach the materials to the substrate. The use of polymeric binders has some drawbacks including increased resistivity and addition of dead weight to the electrode [11]. Previous research has demonstrated that binder-free electrodes show considerably improved performance especially with respect to the power handling of supercapacitor electrodes [12].

It has been demonstrated that thin-film graphene electrodes show exceptional power handling and frequency response [4]. This finding expands the potential applications of supercapacitors as it signals the possibility of high-power supercapacitors that can even replace electrolytic capacitors in certain applications. Miller et al. [4] reported on vertically oriented graphene grown on nickel foil by means of plasma-enhanced chemical vapor deposition (CVD). The supercapacitor showed ac line filtering capability at 120 Hz and a resistance capacitance (RC) time constant of 200 μs. However, the slow graphene growth rate and the use of the vacuum process equipment make this process very costly.

Several methods have been reported to fabricate the binder-free electrodes of graphene nanosheets including the vacuum filtration method [13], CVD [4], electrophoretic deposition (EPD) [14], and layer-by-layer (LBL) assembly [15]. Among these techniques CVD, LBL, and EPD can be easily controlled to deposit a thin film of graphene. However, these methods are time-consuming and costly for industrial production of electrodes. The future application of graphene as supercapacitor material depends on the development of versatile and cost-effective electrode fabrication methods.

In this paper, a versatile and cost-effective technique, electrostatic spray deposition (ESD), has been used to fabricate thin films of graphene. In this method, a liquid precursor solution feeding through a nozzle is atomized at the tip of the nozzle by applying high electric potential between the nozzle and a heated substrate [16–18]. The atomized solution lands on the substrate, and upon evaporation of the solvent, a solid or porous film can be formed. The morphology and thickness of the deposited film can be controlled by adjusting the deposition parameters such as the flow rate, applied potential, substrate temperature, and the composition of the precursor solution [18]. Usually, the precursor is a compound which can be decomposed to the desired material at a high temperature during deposition or calcination after the deposition. For instance ESD has been used to deposit thin films of metal oxides from metal salt solutions [16, 17]. The material to be deposited such as CNT [19] can also be sprayed directly onto the substrate from a suspension of the material in an appropriate solvent. There are few reports in the literature on ESD deposition of graphene and graphene oxide [20, 21]. It was shown that the combination of the small droplet size and rapid evaporation of the solvent upon reaching the preheated substrate avoids the concentration process that takes place upon slow solvent evaporation [21]. This results in reduced restacking graphene sheets during the position and thus provides higher accessibility of the electrodes.

In this study, for the first time, we evaluate the performance of ESD-deposited graphene film for supercapacitor application. A commercially available graphene nanoplatelet (GNP) with medium specific surface area was used as the electrode material. The ESD deposition results in uniform deposited film with an open pore structure. The electrochemical properties of the electrodes were evaluated by cyclic voltammetry (CV), galvanostatic charge–discharge (CD), and electrochemical impedance spectroscopy (EIS). The results show that while the electrodes have an acceptable specific capacitance relative to the medium specific surface area of the starting materials, they show excellent power handling ability and frequency response which is the result of the thin film and open pore structure of the electrodes.

Experimental

GNPs were commercially obtained from Cheaptubes Inc. (Brattleboro, VT, USA). All other chemicals were purchased from Sigma-Aldrich (St Louis, MO, USA). GNPs have a specific surface area of 600–750 m^2 g^{-1} and average platelet diameter of less than 2 μm and were used without any purification. The experimental setup and details of the ESD process used in this work have been reported previously [22]. Figure 1a schematically shows the ESD setup. In typical sample fabrication processes, 6 mg of GNP was added to 20 ml of 1,2-propanediol and sonicated for 30 min with an ultrasonic probe and was placed in an ice bath to form a 0.3-mg ml^{-1} GNP solution. In the next step, the solution was fed to a stainless needle through a syringe pump at a feeding rate of 0.5 or 3 ml h^{-1}, and a voltage of 4–5 kV was applied between the needle and the stainless steel substrate which was placed on a hotplate and heated at

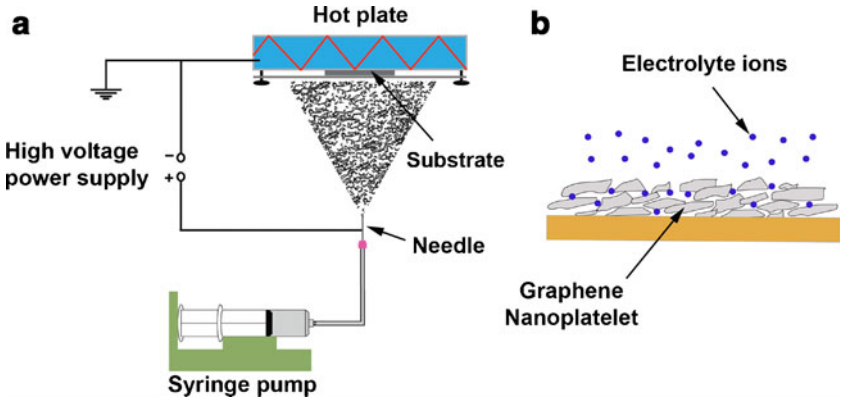

Fig. 1 **a** Schematic drawing of ESD setup that was used in this study. **b** Schematic drawing showing the deposited thin GNP film with open pore structure with easy accessibility of electrolyte ions

250 °C. After the deposition, the thicknesses of the thin films were measured by using a profilometer. The deposition times were adjusted to reach film thicknesses of 1 and 6 μm. Figure 1b schematically shows the structure of deposited GNP films. Electron microscopy was carried out on a JEOL 7000 field emission scanning electron microscope (FE-SEM) and a TECNAI-F20 FEG transmission electron microscope (TEM). The electrochemical tests were carried out on a VMP3 multichannel potentiostat (VMP3; Bio-Logic, USA). The electrochemical performances of the electrodes were studied in a three-electrode cell using a Pt wire and Ag/AgCl electrode as counter and reference electrodes, respectively. A 1 M Na_2SO_4 solution was used as the electrolyte. The EIS measurements were conducted by applying an alternating voltage of 10 mV to the electrode at its open circuit voltage (OCV) from 100 kHz to 50 mHz.

Results and discussion

Figure 2a, b presents the cross-section and top view FE-SEM images of deposited GNP films. As shown in Fig. 2b, GNPs interacted with each other to form an open pore structure, through which electrolyte ions can diffuse and reach the surface of underlying GNPs [23]. Figure 2c shows a TEM image of as-deposited GNPs. It is evident that GNPs are corrugated and scrolled. This is a part of the intrinsic nature of graphene nanosheets, which results from the fact that the 2D membrane structure becomes thermodynamically stable via bending [24]. The as-prepared thin-film GNP electrodes show a moderate specific capacitance with excellent high-power handling. Figure 3a–d shows the CV curves of 1- and 6-μm-thick electrodes at different scan rates ranging from 0.1 to 20 V s^{-1}. Both electrodes show capacitive properties at scan rates as high as 20 V s^{-1}. For the 1-μm-thick electrode, the CV curves exhibit rectangular shapes for scan rates as high as 10 V s^{-1} which shows excellent capacitive properties. At the very high scan rate of 20 V s^{-1}, the shape of CV deviates from the rectangular shape which indicated a more resistive behavior at this scan rate. For the electrode with 6 μm thickness, the CV curves have an ideal rectangular shape at 0.1 and 1 V s^{-1}. However, at scan rates higher than 5 V s^{-1}, the shape of CV curves indicates more resistive contribution of electrodes. At a high scan rate of 20 V s^{-1}, the resistive behavior of the electrodes is dominant and electrodes show small specific capacitance.

At a scan rate of 0.1 V s^{-1}, the specific capacitance of 1-μm-thick electrode is about 52 F g^{-1}. At this scan rate, the specific capacitance of 6-μm-thick electrode is about 49 F g^{-1}. This shows a medium specific capacitance compared to reported data for specific capacitance of graphene (38–264 F g^{-1}). However, it should be noted that the GNP that was used in this study has a medium surface area of 600–750 m^2 g^{-1} and consists of multilayers, and its specific capacitance is reasonable when compared to the reported capacitance of multilayer graphene. It is also worth noting

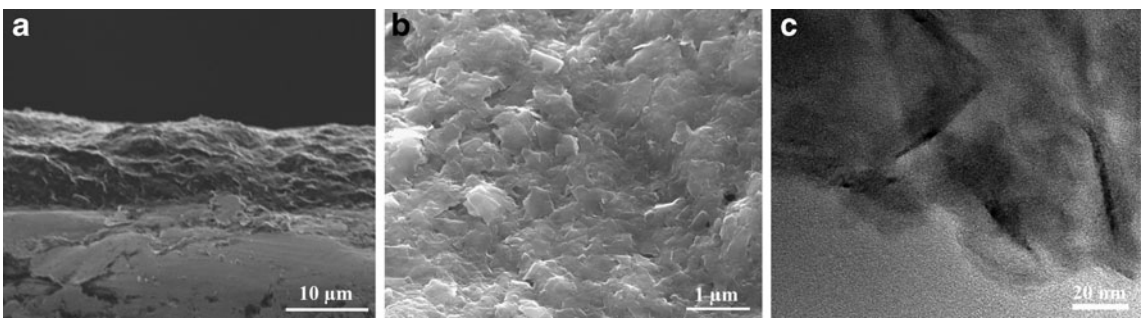

Fig. 2 SEM image of the deposited GNP (6 μm thick) film **a** cross-section view and **b** top view. **c** TEM image of as-received GNP

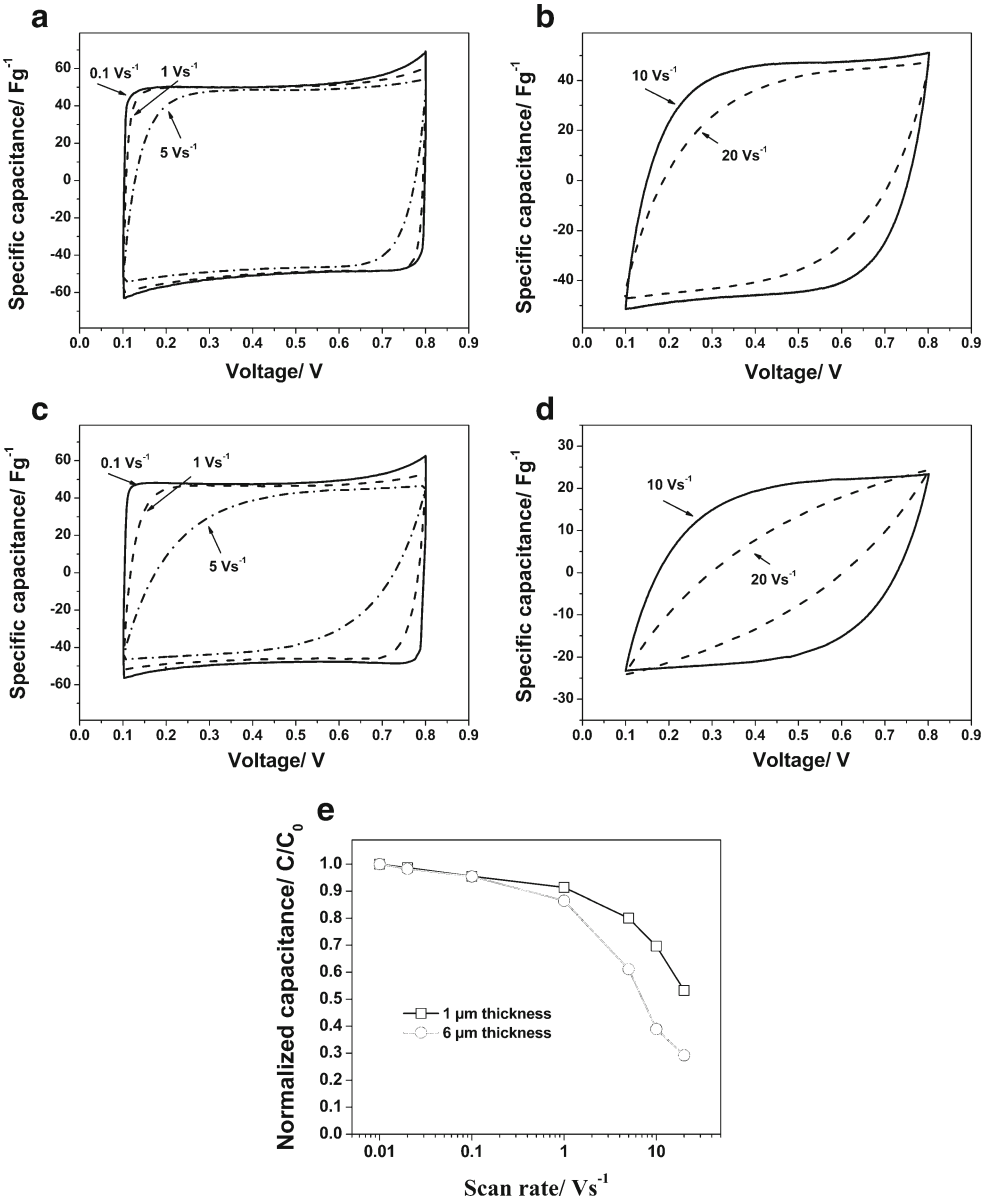

Fig. 3 Cyclic voltammograms recorded in 1 M Na_2SO_4 (vs. Ag/AgCl) of GNP electrodes at various scan rates ranging from 0.1 to 20 V s^{-1} **a**, **b** 1-μm-thick electrode and **c**, **d** 6-μm-thick electrode. **e** Plot of normalized capacitance vs. scan rate for electrodes with 1 and 6 μm thickness

that in the process of making the graphene film electrodes, no surfactant materials were used to disperse the graphene in the deposition solution. Recently, Brownson et al. [25] showed that the presence of surfactant could affect the specific capacitance of graphene electrodes. For instance, the specific capacitance of about 148 F g^{-1} for graphene dispersed in the processing solution with the help of surfactant and tested in 1 M H_2SO_4 electrolyte dropped to about 63 F g^{-1} without using the surfactant [25].

To investigate the rate capability of graphene film electrodes, the normalized specific capacitance of the films at scan rates between 0.01 and 20 V s^{-1} was calculated and shown in Fig. 3e. The drop in capacitance of the thinner electrode with respect to specific capacitance at 0.1 V s^{-1} is only 20 % at a high scan rate of 5 V s^{-1}. The drop in capacitance at a 5 V s^{-1} scan rate is higher for the thicker electrode (38 %) but is still lower than most of the reported thin-film electrodes. For both electrodes the capacitance drops slowly with further increase in the scan rate, and at a very high scan rate of 20 V s^{-1}, around 53 % of specific capacitance of electrodes with 1 μm thickness and 30 % of the specific capacitance of the electrodes with 6 μm thickness are retained. These results show the excellent rate capability and power handling of graphene thin-film electrodes. Moreover, it can be concluded that the thickness of the electrode has strong influence on the power handling ability and highlights the importance of thin-film electrodes for applications that require high-rate capability.

The properties of the thin-film electrodes were also studied by galvanostatic CD tests. Figure 4a–d shows charge/discharge curves of the electrodes at various current densities. At all current densities, the curves show triangular shapes indicating ideal capacitive behavior. The *iR* drop, the sudden

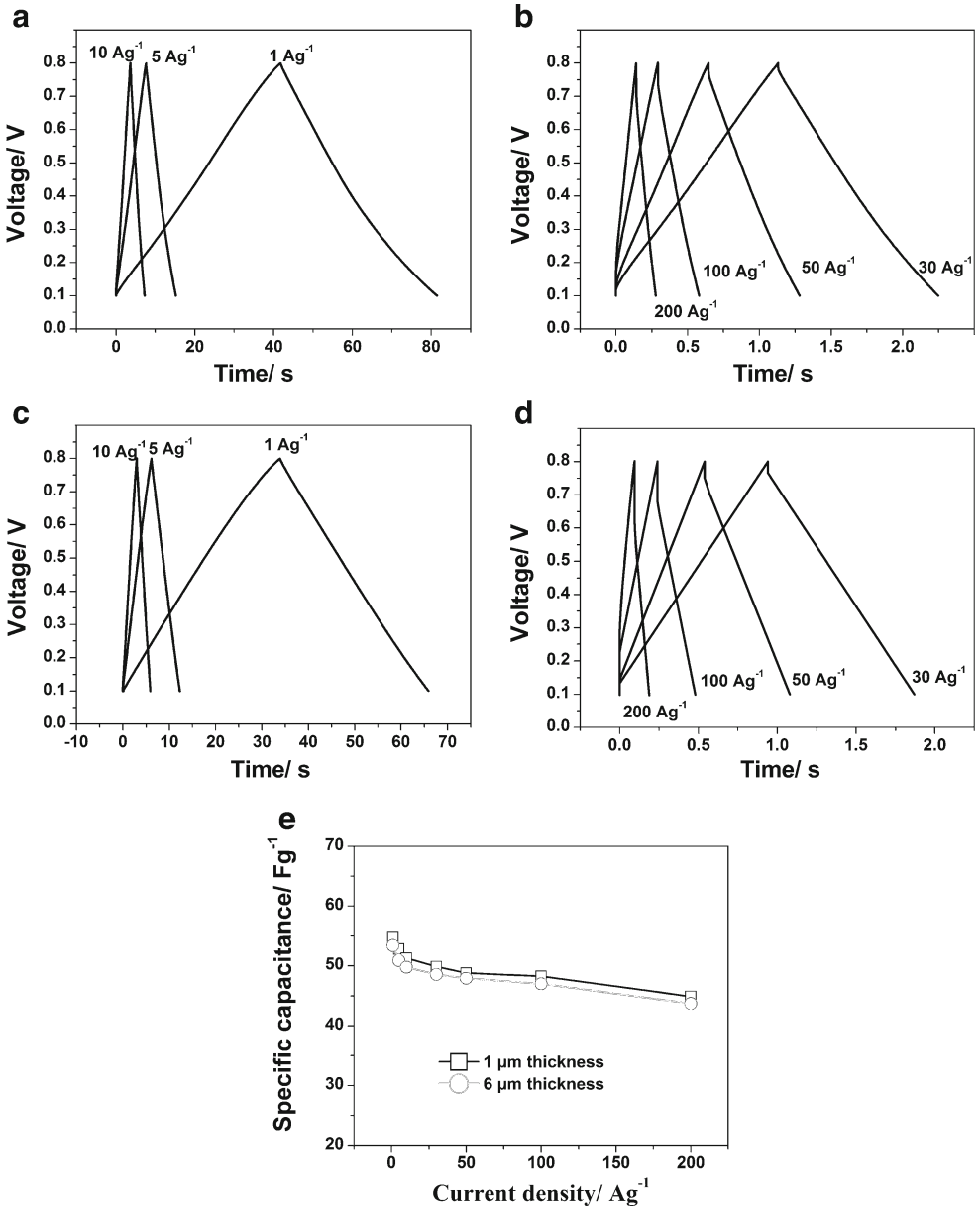

Fig. 4 Galvanostatic charge/discharge curves of GNP thin-film electrode at various current densities ranging from 1 to 200 A g^{-1} **a**, **b** 1-μm-thick electrode and **c**, **d** 6-μm-thick electrode. **e** Specific capacitances obtained from galvanostatic charge/discharge measurements at various current densities

voltage drop at the beginning of discharge curves, is very small for both types of electrodes at low discharge current densities of 1–10 A g^{-1}. At higher discharge current densities, the *iR* drop increases but is still relatively small. At a discharge current density of 50 A g^{-1}, the *iR* drop for the electrode with 1 μm thickness is about 0.03 V and it increases to 0.09 V at a higher discharge current density of 200 A g^{-1}. It should be noted that a discharge current density of 200 A g^{-1} is much higher than discharge rates that are usually used to test the supercapacitor electrodes (between 0.1 and 10 A g^{-1}) [26]. Figure 4d presents the specific capacitance of the electrodes at various discharge current densities. At the low discharge rate of 1 A g^{-1}, the specific capacitance of the GNP films with 1 and 6 μm thicknesses are about 55 and 53 F g^{-1}, respectively. For both electrode thicknesses, approximately 82 % of the specific capacitance at the 1-A g^{-1} discharge rate was recorded at a very high discharge rate of 200 A g^{-1}. These results, in agreement with results obtained from cyclic voltammetry, confirm exceptional high-rate handling ability of the GNP films fabricated through the ESD technique. The rate capability of GNP film electrodes is very similar to that of onion-like carbon (OLC) which has lower specific capacitance compared to GNP (≤40 F g^{-1}) [11, 12, 27].

Further investigation of electrodes was performed using EIS. For a more informative analysis of EIS results, we transformed the impedance data to the complex capacitance following the approach that is described by Taberna et al. [28]. In this approach, the real part (C') and the imaginary part (C'') of the capacitance are both a function of the frequency and can be

extracted from impedance data according to Eqs. (1) and (2) [28, 29].

$$C'' = \frac{Z'(f)}{2\pi f|Z(f)|^2} \tag{1}$$

$$C' = \frac{Z''(f)}{2\pi f|Z(f)|^2} \tag{2}$$

where $Z(f)$ is the complex impedance at frequency f, and $Z'(f)$ and $Z''(f)$ are real and imaginary part of the complex impedance, respectively.

Figure 5a, b show the resulting graphs for the electrodes with 1 and 6 μm thickness, respectively. For the real part of the capacitance, an increase in capacitance is observed with a decrease in ac frequency and the capacitance value approaches to the value obtained from CV tests. For imaginary capacitance plots, a peak shape curve is obtained. The rate capability of the electrode can be characterized in the real capacitance plots by observing the frequency range where the capacitance increases. The rate capability can also be quantitatively evaluated from the frequency of the capacitive peak in imaginary capacitance plots [30]. This characteristic frequency (f_0) marks the point at which the phase angle of the impedance is −45° (resistive and capacitive impedance are equal), and the electrode is discharged at 50 % efficiency [27, 28]. The characteristic frequency was estimated to be around 28 and 17 Hz for the electrodes with 1 and 6 μm thicknesses, respectively. The corresponding time constants τ_0 ($\tau_0 = 1/f_0$) were about 36 and 59 ms, respectively. For comparison, it is worth noting that many of the reported supercapacitor electrodes with high-rate capability have much higher time constants. For instance, the calculated time constant in aqueous electrolyte is 700 ms for MCNT [27], 1.1 s for OLC [27], and 379 ms for carbide-derived carbon (CDC) nano-felts [11]. There are some reports in the literature about supercapacitor devices with lower RC time constants. A 7-μm-thick film of OLC arranged in

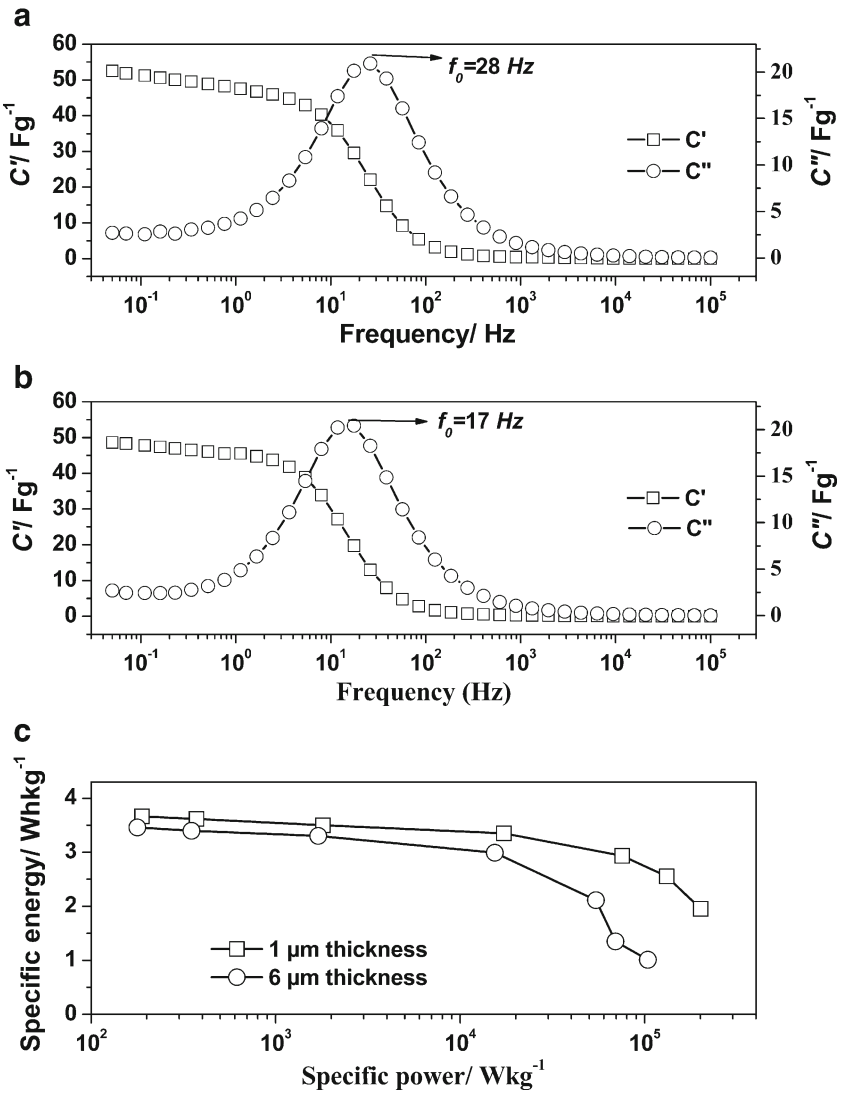

Fig. 5 Plots of complex real (C') and imaginary (C'') capacitance as a function of frequency for **a** electrode with 1 μm thickness and **b** electrode with 6 μm thickness. The EIS measurements were conducted in 1 M Na_2SO_4 at OCV by applying an alternating voltage of 10 mV. **c** Plots of utilizable specific energy vs. power density (Ragone plot) of the thin-film GNP electrodes. The energy and power densities are calculated from CV results at scan rates ranging from 0.1 to 20 V s^{-1}

interdigital micro-supercapacitor device showed a 26-ms RC time constant [12]. However, OLCs have lower specific capacitance compared to GNPs that are used here (<40 F g^{-1}). To the best of our knowledge, the highest rate capability that has been reported so far is for that of supercapacitor with 0.6-μm-thick vertically oriented graphene sheets that could achieve a time constant of 200 μs at a high frequency of 120 Hz. At this frequency the capacitance of a device with a 2-cm^2 surface area was 175 μF, making the capacitance of a single electrode about 359 μF (normalized capacitance of 175 μF cm^{-2}). It is worth noting that at higher frequencies of 125 Hz, the supercapacitor electrodes reported in this study show a normalized capacitance of 850 and 2,000 μF cm^{-2} for the film thickness of 1 and 6 μm, respectively. Table 1 compares the reported RC time constant and specific capacitance of electrodes that are reported in this work to some of the supercapacitor electrodes with high-frequency response that are reported in the literature.

A combination of the binder-free deposition technique, the thin-film configurations of GNPs with an open pore structure, and the high conductivity of GNPs are responsible for the observed high-power handling ability of the electrodes. A Ragone plot calculated from CV results [12] (Fig. 5c) reveals that the 1-μm-thick electrode shows a specific energy of 3.66 W h kg^{-1} at a 188.50-W kg^{-1} specific power. The specific energy slowly decreases as specific power increases and at a very high specific power of 200.90 kW kg^{-1}, the specific energy of 1.95 W h kg^{-1} was achieved. The cyclic performance of a thin-film electrode was tested by cyclic voltammetry at 0.1 V s^{-1}. As shown in Fig. 6, after 5,000 cycles, about 94 % of the initial capacitance of the electrode was retained which shows excellent cycling stability of the electrode.

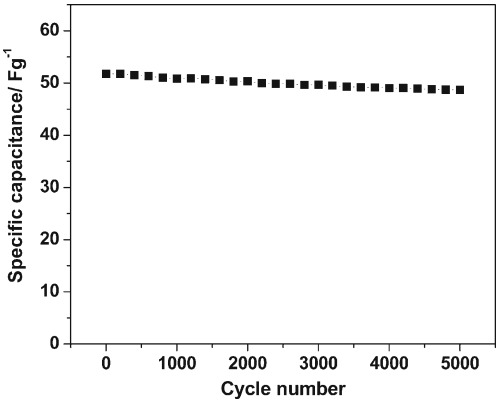

Fig. 6 Cyclic stability of a 1-μm-thick electrode tested at a 0.1-V s^{-1} CV scan rate in 1 M Na_2SO_4 electrolyte

Conclusions

In summary, for the first time, we have utilized the ESD technique to fabricate binder-free thin films of GNP for supercapacitor application. A commercially available multilayer GNP was selected to demonstrate the fabrication technique. The electrodes show excellent high-rate handling ability as it was shown by various electrochemical testing techniques. Electrodes with 1 μm thickness show a much better rate handling ability compared to electrodes with 6 μm thickness, highlighting the effect of electrode thickness on the power performance of supercapacitors. At the low discharge rate of 1 A g^{-1}, the specific capacitance of the GNP films with 1 and 6 μm thicknesses is about 55 and 53 F g^{-1}, respectively. The specific capacitance of the electrodes is lower than that of the high-quality, lab-produced single-layer graphene. We anticipate that by using graphene materials with higher surface areas and optimizing the deposition conditions, higher specific capacitance is feasible. Nonetheless, the GNP electrodes studied here are an excellent candidate for the applications that require high power and moderate energy density. EIS experiments indicate excellent frequency response of the electrodes, and the low RC time constants of 36 and 59 ms were recorded for electrodes with 1 and 6 μm thickness, respectively. Additionally, the demonstrated fabrication process (ESD) is a low-cost technique that could potentially be employed to fabricate thin-

Table 1 Comparison of RC time constant and specific capacitance of the thin-film GNP electrodes to some of the electrodes with high-frequency response that are reported in the literature

Electrode materials	Voltage for EIS test (V)	Voltage amplitude for EIS (mV)	Electrolyte	RC time constant (s)	Specific capacitance	Reference
MWCNT	0	5	1.5 M NEt_4BF_4 in acetonitrile	0.7	~20 F g^{-1} at 5 mA cm^{-2}	[27]
OLC	0	5	1.5 M NEt_4BF_4 in acetonitrile	1.1	~25 F g^{-1} at 5 mA cm^{-2}	[27]
TiC-CDC nanofelt	N/A	N/A	1 M H_2SO_4	0.379	108 F g^{-1} at 5 mA cm^{-2}	[11]
OLC micro-supercapacitor	OCV	10	1 M Et_4NBF_4 in PC	0.026	1.7 mF cm^{-2} at 1 V s^{-1}	[12]
AC micro-supercapacitor	OCV	10	1 M Et_4NBF_4 in PC	0.7	11.6 at 500 mV s^{-1}	[12]
Vertically oriented graphene sheets	N/A	N/A	25 % KOH	0.0002	175 μF cm^{-2} at 120 Hz	[4]
Thin GNP electrodes (1 μm)	OCV	10	1 M Na_2SO_4	0.036	55 F g^{-1} at 1 A g^{-1}, 850 μF cm^{-2} at 125 Hz	This work
Thin GNP electrodes (6 μm)	OCV	10	1 M Na_2SO_4	0.059	53 F g^{-1} at 1 A g^{-1}, 2,000 μF cm^{-2} at 125 Hz	This work

film electrodes of various kinds of graphene and its composites.

Acknowledgments MB acknowledges financial support from DEA fellowship, Florida International University. The authors acknowledge the staff of FIU clean-room facility.

References

1. Conway BE (1997) Electrochemical supercapacitors: scientific fundamentals and technological applications. Kluwer/Plenum, New York
2. Miller JR, Burke AF (2008) Electrochemical capacitors: challenges and opportunities for real-world applications. Electrochem Soc Interface 1:53–57
3. Simon P, Gogotsi Y (2008) Materials for electrochemical capacitors. Nat Mater 7:845–854
4. JR Miller J, Outlaw RA, Holloway BC (2010) Graphene double-layer capacitor with ac line-filtering performance. Science 329:1637–1639
5. Pandolfo A, Hollenkamp A (2006) Carbon properties and their role in supercapacitors. J Power Sourc 157:11–27
6. Obreja V (2008) On the performance of supercapacitors with electrodes based on carbon nanotubes and carbon activated material—a review. Physica E 40:2596–2605
7. Brownson DAC, Kampouris DK, Banks CE (2011) An overview of graphene in energy production and storage applications. J Power Sourc 196:4873–4885
8. Wang HW, Hu ZA, Chang YQ, Chen YL, Lei ZQ, Zhang ZY, Yang YY (2010) Facile solvothermal synthesis of a graphene nanosheet–bismuth oxide composite and its electrochemical characteristics. Electrochim Acta 55:8974–8980
9. Lu T, Zhang Y, Li H, Pan L, Li Y, Sun Z (2010) Electrochemical behaviors of graphene–ZnO and graphene–SnO_2 composite films for supercapacitors. Electrochim Acta 55:4170–4173
10. Wu ZS, Ren W, Wang DW, Li F, Liu B, Cheng HM (2010) High-energy MnO_2 nanowire/graphene and graphene asymmetric electrochemical capacitors. ACS Nano 4:5835–5842
11. Presser V, Zhang L, Niu JJ, McDonough J, Perez C, Fong H, Gogotsi Y (2011) Flexible nano-felts of carbide-derived carbon with ultra-high power handling capability. Adv Energ Mater 1:423–430
12. Pech D, Brunet M, Durou H, Huang P, Mochalin V, Gogotsi Y, Taberna PL, Simon P (2010) Ultrahigh-power micrometre-sized supercapacitors based on onion-like carbon. Nat Nanotechnol 5:651–654
13. Yu A, Roes I, Davies A, Chen Z (2010) Ultrathin, transparent, and flexible graphene films for supercapacitor application. Appl Phys Lett 96:253105
14. Chen Y, Zhang X, Yu P, Ma Y (2010) Electrophoretic deposition of graphene nanosheets on nickel foams for electrochemical capacitors. J Power Sourc 195:3031–3035
15. Byon HR, Lee SW, Chen S, Hammond PT, Shao-Horn Y (2010) Thin films of carbon nanotubes and chemically reduced graphenes for electrochemical micro-capacitors. Carbon 49:457–467
16. Sokolov S, Paul B, Ortel E, Fischer A, Kraehnert R (2011) Template-assisted electrostatic spray deposition as a new route to mesoporous, macroporous, and hierarchically porous oxide films. Langmuir 27:1972–1977
17. Yu Y, Gu L, Dhanabalan A, Chen CH, Wang C (2009) Three-dimensional porous amorphous SnO_2 thin films as anodes for Li-ion batteries. Electrochim Acta 54:7227–7230
18. Jaworek A, Sobczyk AT (2008) Electrospraying route to nanotechnology: an overview. J Electrost 66:197–219
19. Kim J, Nam K, Ma S, Kim K (2006) Fabrication and electrochemical properties of carbon nanotube film electrodes. Carbon 44:1963–1968
20. Han P, Yue Y, Liu Z, Xu W, Zhang L, Xu H, Dong S, Cui G (2011) Graphene oxide nanosheets/multi-walled carbon nanotubes hybrid as an excellent electrocatalytic material towards VO^{2+}/VO_2^+ redox couples for vanadium redox flow batteries. Energy Environ Sci 4:4710–4717
21. Gilje S, Han S, Wang M, Wang KL, Kaner RB (2007) A chemical route to graphene for device applications. Nano Lett 7:3394–3398
22. Chen W, Beidaghi M, Penmatsa V, Bechtold K, Kumari L, Li WZ, Wang C (2010) Integration of carbon nanotubes to C-MEMS for on-chip supercapacitors. IEEE Trans Nanotechnol 9:734–740
23. Lv W, Tang D-M, He Y-B, You C-H, Shi Z-Q, Chen X-C, Chen C-M, Hou P-X, Liu C, Yang Q-H (2009) Low-temperature exfoliated graphenes: vacuum-promoted exfoliation and electrochemical energy storage. ACS Nano 3:3730–3736
24. Wang G, Shen X, Yao J, Park J (2009) Graphene nanosheets for enhanced lithium storage in lithium ion batteries. Carbon 47:2049–2053
25. Brownson DAC, Banks CE (2012) Fabricating graphene supercapacitors: highlighting the impact of surfactants and moieties. Chem Comm 48:1425–1427
26. Wang G, Zhang L, Zhang J (2011) A review of electrode materials for electrochemical supercapacitors. Chem Soc Rev 41:797–828
27. Portet C, Yushin G, Gogotsi Y (2007) Electrochemical performance of carbon onions, nanodiamonds, carbon black and multiwalled nanotubes in electrical double layer capacitors. Carbon 45:2511–2518
28. Taberna PL, Simon P, Fauvarque JF (2003) Electrochemical characteristics and impedance spectroscopy studies of carbon–carbon supercapacitors. J Electrochem Soc 150:A292
29. Jang JH, Yoon S, Ka BH, Jung YM, Oh SM (2005) Complex capacitance analysis on leakage current appearing in electric double-layer capacitor carbon electrode. J Electrochem Soc 152: A1418–A1422
30. Jang JH, Kato A, Machida K, Naoi K (2006) Supercapacitor performance of hydrous ruthenium oxide electrodes prepared by electrophoretic deposition. J Electrochem Soc 153:A321–A328